



Contents lists available at ScienceDirect

Surface & Coatings Technology

journal homepage: www.elsevier.com/locate/surfcoat

Growth kinetics of plasma deposited microcrystalline silicon thin films

E. Amanatides, D. Mataras*

Plasma Technology Laboratory, Department of Chemical Engineering, University of Patras, P.O. Box 1407, 26504 Patras, Greece

ARTICLE INFO

Article history:

Received 16 September 2010

Accepted in revised form 15 December 2010

Available online xxxx

Keywords:

Microcrystalline silicon

Nanostructure

Solar cells

Simulation

PECVD

ABSTRACT

A continuum model for the nucleation and growth of microcrystalline silicon thin films from SiH_4/H_2 discharges is presented. The simulation considers mass balances and surface coverage with adspecies and silicon clusters up to the size where they can be considered as thermodynamically stable. The model is combined to a plasma gas phase simulator and a simulator of thin film morphology and is used for studying the growth differences in two different regions, the center and the edge of a $30 \times 30 \text{ cm}^2$ substrate. The predictions for the film growth rate, film crystallinity and surface roughness in both regions are presented and discussed together with the main processes governing nucleation and growth and the slow step for stable nanocrystal formation.

© 2010 Elsevier B.V. All rights reserved.

1. Introduction

Hydrogenated microcrystalline silicon ($\mu\text{-Si:H}$) is a key material for thin film solar cells in the current industrial practice [1]. This material is commonly produced using Plasma Enhanced Chemical Vapor Deposition (PECVD), from highly diluted SiH_4 in H_2 discharges [2]. Several theoretical models have been proposed concerning the growth of this material and especially the mechanism of nanocrystal formation under the rather low PECVD temperatures [3–6]. All of them are based on experimental observations and define the conditions that need to be fulfilled for crystallization to take place. However, it has become clear in recent years that for understanding low temperature nucleation and nanocrystal formation an integrated model is needed including gas phase and surface processes along with the energy transfer to the surface by plasma species.

This work presents an effort to create a continuum model for the nucleation and growth of $\mu\text{-Si:H}$ thin films based on the mass balances and the surface coverage of adspecies and clusters. The model follows the formation and evolution of silicon nuclei up to a critical size and is combined to a gas phase simulator in order to develop a complete simulation tool for the $\mu\text{-Si:H}$ deposition process, capable to predict the plasma properties, the deposition rate, film crystallinity and morphology. The gas phase and the surface model are applied in typical deposition conditions of $\mu\text{-Si:H}$ that lead to high quality material for solar cells in a medium scale plasma reactor. The main differences in nucleation and growth of the film deposited in the center and on the edge of the substrate holder are discussed together with the mechanism for stable nanocrystal formation.

2. Theory/calculation

2.1. Gas phase model description

A two dimensional (2D), time dependent fluid model was used to study the process drifts during $\mu\text{-Si:H}$ deposition from high pressure–high power 40.68 MHz SiH_4/H_2 discharges. Briefly, the model describes the discharge using a combination of particle, momentum and electron energy conservation equations derived from the Boltzmann equation, coupled with Poisson's equation for a self-consistent calculation of the electric field. A detailed description of the model can be found elsewhere [7]. A set of 25 species (neutrals, radicals, positive and negative ions) together with a total number of 85 gas phase reactions are included into the gas phase chemistry model. The reactions include electron-impact collisions with molecular species, radical–molecule, radical–radical, positive ions–neutral, negative ion–neutrals, and ion recombination reactions. Cross section data are used for the electron impact reactions, whereas the rate constants of the rest of the reactions involving neutral species are either calculated or experimentally measured. The collision cross section data and the rate constants of the reactions were taken from Ref. [8–10]. Plasma surface interaction of radicals and radical/ion/atom fluxes towards the surface was calculated using sticking coefficients [8]. Time steps of 10^{-9} , 10^{-6} , and 10^{-3} sec were successively used in order to be able to simulate real deposition times of a few minutes in reasonable computational times. In order to avoid divergence due to plasma module instabilities when solving for time steps $> 10^{-6}$ s, the whole problem was solved once every 1000 iterations with the smallest time step of 10^{-9} s. This approach allowed us to get stable solutions for real deposition times of 1800 s. The time variation of the main species fluxes, the energy transferred to the surface and the deposition rate in the center and on the edge of

* Corresponding author. Tel.: +30 2610969525/993361.

E-mail address: dim@plasmatech.gr (D. Mataras).

a 30 × 30 cm² substrate holder were recorded and used as an input for the surface model.

2.2. Model for film nucleation and growth

The simulation of the nucleation and growth of the films was performed by solving the balance equations for adspecies and clusters formed on the surface [11]:

$$\frac{d\theta_n}{dt} = F\theta_{n-1} + \sum_{i=1,n} v'(i)\theta_{n-i}\theta_i - \sum_{i=1,n} v'(i)\theta_n\theta_i - \sum_{i=1,n} D(i)\theta_n\theta_i - F\theta_n \quad (1)$$

where *F* is the species flux from the gas phase model, θ_i is the surface coverage with clusters of *i* silicon atoms, *n* is the number of silicon atoms in a nucleus of a critical nucleus size, *v'(i)* is the frequency of attachment of adspecies or clusters to another cluster, and *D(i)* is the diffusion coefficient of an adspecies or cluster to another cluster. The left hand term of Eq. (1) accounts for the accumulation of adspecies or clusters on the surface, while the right hand term for the production and annihilation of different sites either coming from the gas phase species or from reaction and diffusion on the surface. The system of the balance equations is closed by considering that the sum of the surface sites coverage at each time step is equal to unity

$$\sum_{i=1,n} \theta_i = 1 \quad (2)$$

The mass balances equations was solved for a 50 × 50 nm surface and a time step equal to the one of the gas phase model. We have used an adspecies discretization scheme, which leads to an initial grid of a 20,000 tetragonal cells, which is continuously deforming in relation with the cluster size.

The critical nucleus size i.e. the minimum nucleus radius that is thermodynamically stable was calculated from the variation of the Gibbs free energy change for the system glass – film – vacuum according to the equation [12]:

$$\Delta G = a_3 r^3 \Delta G_v + a_1 r^2 \gamma_{fv} + a_2 r^2 \gamma_{fs} - a_2 r^2 \gamma_{sv} \quad (3)$$

where, ΔG_v is the Gibbs free energy change at a constant volume, *r* is the nucleus radius, $\alpha_1, \alpha_2, \alpha_3$ are geometric terms, γ_{sv} , γ_{fs} and γ_{fv} are the surface tensions for the substrate-vapor, film-substrate and film-vapor respectively. For glass/silicon - vacuum interface tensors γ_{sv} and γ_{fv} , typical values of 0.45 and 1.23 J/m² have been used. For the glass-silicon interface tensor γ_{fs} in order to simulate conditions of the initial growth stage we have used a value of 0.2 J/m², which corresponds to a de-bonded glass-silicon interface [13]. In addition, for the specific system and the estimated values of γ_{sv} , γ_{fs} and γ_{fv} the geometric factors α_1, α_2 and α_3 have been computed to 4.97, 3.01 and 1.45, while ΔG_v to 9.48 × 10⁸ J/m³.

It is worth noting that for our system glass – Si film – vapor $\gamma_{sv} < \gamma_{fs} + \gamma_{fv}$, which means that initially the film will follow a Vollmer-Weber growth mode and will favor the formation of 3d islands [12]. However, the value of γ_{sv} will continuously change as the glass substrate will be covered with silicon leading to a Stranski-Krastanov growth mode [12].

Fig. 1 presents the variation of ΔG as a function of the nucleus diameter as calculated from Eq. (3). The critical nucleus radius is calculated in the equilibrium condition $d\Delta G/dr = 0$ according to the equation:

$$r^* = \frac{-2(\alpha_1 \gamma_{fv} + a_2 \gamma_{fs} - a_2 \gamma_{sv})}{3\alpha_3 \Delta G_v} \quad (4)$$

which for the specific system gives a value of 2.6 nm.

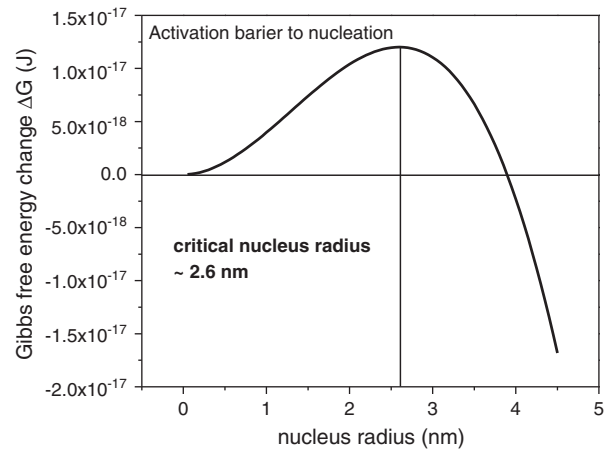


Fig. 1. Gibbs free energy change as a function of nucleus radius for the system glass – Si film – vacuum.

The energy per nucleus area should be transferred from the plasma phase in order to ensure the formation of stable nanocrystals. If a stable cluster is formed then it will continue to grow without any energy barrier as we can see from the variation of ΔG in Fig. 1.

Finally, the prediction of film morphology and roughness is achieved by solving together with the site balance equations, the differential equation for the film height *h* [14]:

$$\frac{dh(y_i, t)}{dt} = \begin{cases} = 0, & \text{if } \Delta h > \frac{y_i - y_{i-1}}{\tan\theta} \\ = \bar{R} + (\sqrt{2}-1) \cdot r(y_i, t) & \text{if } \Delta h \leq \frac{y_i - y_{i-1}}{\tan\theta} \end{cases} \quad (5)$$

where, the term \bar{R} captures the average film growth rate due to the flux of species towards the surface, $r(y_i, t)$ is the nucleus radius at the position y_i and time *t*, θ is the species angle of incidence and Δh is the film height difference between grid point y_i and y_{i-1} at specific time *t*. In fact, these height correction terms in the present state of the model account for: (a) shadowing effects due to the species angle of incidence and (b) a cluster shape correction factor in order to transform the calculated cubic shape of the nucleus to a spherical one.

3. Results and discussion

The gas phase and surface models were applied in a medium scale (30 × 30 cm² substrate size) plasma reactor that is typically used for the production of micromorph tandem solar devices. The reactor is equipped with a showerhead and pumping slits for ensuring a uniform gas distribution. The simulated geometry has been described in detail in Ref. [15]. The deposition conditions were: total gas pressure 6 mbar, 6% SiH₄ in H₂, 1 slm total gas flow, power = 250 Watt and frequency 40.68 MHz. The experimentally measured average deposition rate was 5.5 Å/sec and the crystalline volume fraction of the deposited material in the center was 55% while on the edge the material remains amorphous.

Fig. 2(a) presents the time variation of SiH₂ and SiH₃ fluxes towards the center and the edge of the 30 × 30 cm² substrate. There is a continuous increase of the species flux and a steady state is not reached even after 600 s of deposition. In addition, the flux of SiH₂ and SiH₃ is always higher in the center of the electrode than on the edge.

This continuous change of almost all plasma properties during the film deposition has been also observed by other groups [16,17]. In fact the model predicts a temperature rise in the bulk of the plasma due to the heat release of exothermic reactions of the heavy species. The heat is also transferred towards the substrates but this is a rather slow step. Temperature equilibrium is not reached even after 600 s of deposition

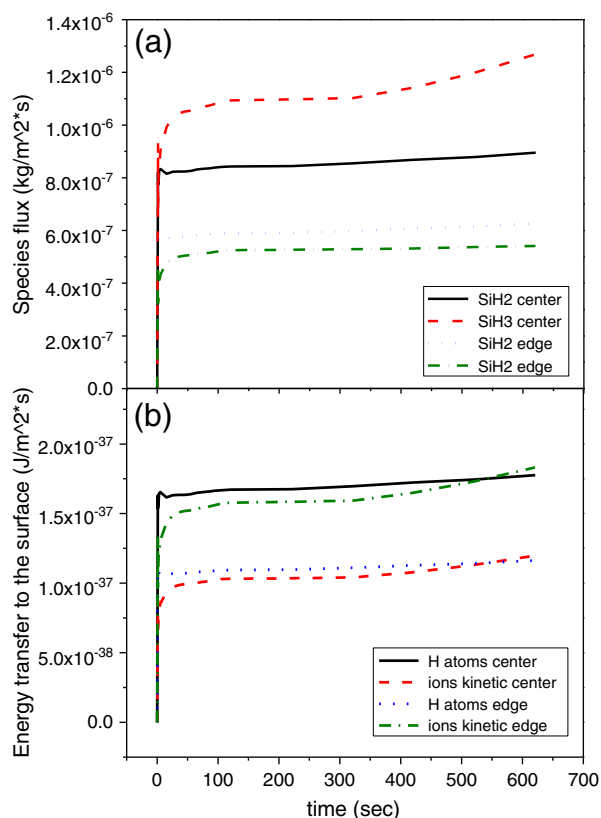


Fig. 2. (a) Species fluxes towards the center and the edge of the substrate holder as a and (b) Energy transfer from H atoms and ions towards the center and the edge of the substrate holder as a function of the deposition time.

and the species fluxes increase, due to the enhancement of the diffusion coefficient with temperature.

Moreover, the flux of species in the center of the substrate is higher compared to the one on the edge. On the edge of the RF electrode and substrate holder the electric field intensity is very strong and this favors SiH₄ and H₂ ionization instead of dissociation. Thus, the initial production and subsequently the flux of neutral species become lower in this region. As a result the model predicts a deposition rate of 5 Å/s in the center and 4.2 Å/s on the edge.

Fig. 2(b) presents the energy transfer towards the surface due to H atoms and ions as a function of the deposition time. The amount of energy transferred to the surface, calculated according to Ref. [18], is very important as it can speed up and favor the formation of stable nuclei. As in the case of species fluxes there is a continuous drift of the energy transfer mainly due to the variation of the species/ions fluxes. The total amount of energy is slightly higher in the center than on the edge because of the much higher H atoms flux there. On the edge, the energy transfer due to ions dominates because of the higher ionization rate in this area as well as the enhanced acceleration of positive ions towards the surface from the electric field.

The variation of species fluxes and the energy transferred to the surface were used as inputs of the nucleation and growth model. Thus, Fig. 3 presents the frequencies of the events that lead to an increase of cluster size as a function of nucleus radius. The dashed line corresponds to the increase of cluster size due to species arrival from the gas phase, while the solid line follows processes that take place on the surface (adspecies–cluster and cluster–cluster reactions). We can distinguish three different regions of nuclei growth: (a) at the early stage of deposition when the size of nuclei is small (<0.5 nm) surface clustering is favored, (b) for nuclei radius between 0.5 nm and 3 nm, where the increase of nucleus size takes place mainly because of the species arrival from the gas phase and (c) for nuclei sizes higher

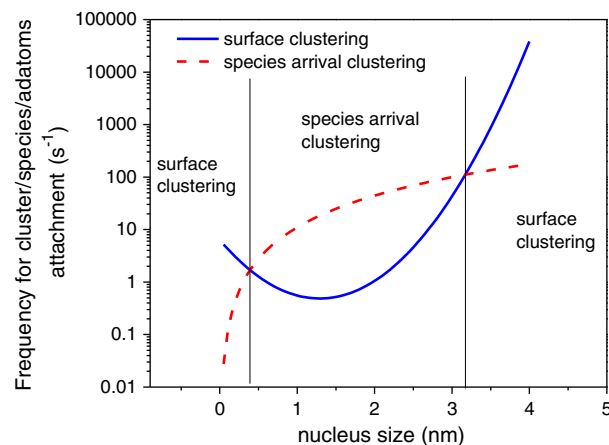


Fig. 3. Frequencies for species/adspecies clustering as a function of the nucleus size.

than 3 nm where surface clustering is almost spontaneous. Moreover, the frequencies for attachment and adspecies clustering are much lower at the early stage of the deposition and this is the slow and critical step for the formation or not of microcrystalline silicon. In fact, the higher the amount of energy that is transferred from the plasma to the surface the higher the frequencies of events that lead to the increase of cluster size.

Fig. 4 presents the fraction of adspecies and clusters of critical size during 600 s of deposition in the center of the electrode (a) and on the edge (b). At the early stage of deposition the surface is fully covered with adspecies and after 15 s in the center of the electrode the first stable nuclei appear. This considering the film growth rate means that a layer of 8 nm is formed before the first stable nanocrystals appear. On the edge the nucleation is delayed and the first stable nuclei

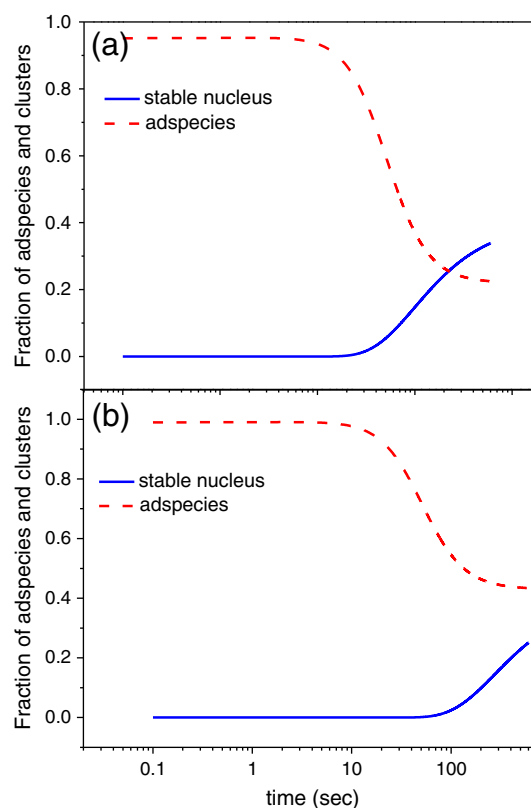


Fig. 4. Fraction of adspecies and clusters of critical size as a function of the deposition time in (a) the center of the electrode and (b) the edge.

appear after 45 s of deposition, which corresponds to a layer of about 20 nm. The difference between center and edge is explained if we take into account the lower frequencies for clustering on the edge because, as shown previously, the rate of species arrival and the energy transferred to the surface is lower there. After 600 s of deposition the surface coverage with stable nuclei in the center of the electrode is about 40% while on the edge is about 20%.

The different nucleation rate in the center of the electrode and on the edge is also reflected in the calculated % crystalline volume fraction which is presented in Fig. 5(a) as a function of the deposition time. The % crystalline volume fraction was estimated using the relation:

$$\% \text{crystallinity} = \frac{\text{volume occupied by stable crystals}}{\text{total film volume}} \times 100 \quad (6)$$

After 600 s of deposition, the model predicts a crystalline volume fraction of 25% in the center of the electrode and about 12% in the edge. We underestimate the experimentally measured film crystallinity in the center (55%) because currently the model does not consider nanocrystals with size larger than the critical size. Once such stable nuclei have been formed, their size will increase rapidly through attachment of smaller clusters to them as this process is thermodynamically favored. In addition, the gas phase model does not include the formation of nanoparticles in the gas phase and consequently a possible participation to the film growth. Their role can be important under certain conditions in the nucleation and formation of stable crystals and will be included in future model updates. On the other hand, we overestimate the experimentally measured crystalline volume fraction on the edge probably because possible sputtering effects have also not been included in this version

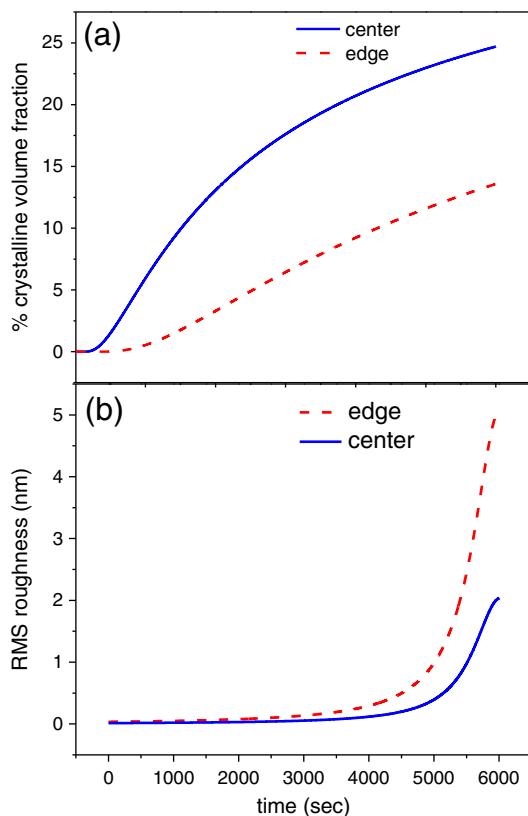


Fig. 5. (a) % crystalline volume fraction in the center and the edge of the deposition electrode and (b) RMS surface roughness in the center and the edge of the substrate holder as a function of the deposition time.

of the model. High energy ions that bombard the surface in this area can break or terminate cluster growth resulting to amorphous material.

Finally, Fig. 5(b) presents the RMS roughness of the surface as a function of the deposition time in the center and on the edge of the electrode. After 600 s of deposition the model predicts a roughness of about 2 nm in the center of the electrode and about 5 nm on the edge. During the early stage of deposition, surface roughening is mostly due to the formation of nuclei of different sizes. As the process is evolving, the material on the edge grows rougher because of the change in the average angle of incidence of the species. In fact, in the center of the electrode the gas phase model predicts an almost 90° angle of incidence. However, on the edge of the electrode the angle of incidence is about 80° because of the adjacent dead volume to the reactor walls, which enhances the species diffusive flux parallel to the surface. The distortion in the angle of incidence produces shadowing effects that lead to the calculated rise of surface roughness.

4. Conclusions

A continuum model for the nucleation and growth of microcrystalline silicon thin films was developed and combined to a simulator of the gas phase. Mass balances of adspecies and clusters on the surface were used to monitor the formation of small clusters up to stable nuclei along with the solution of a partial differential equation involving the surface height to follow the film morphology.

According to the frequencies for cluster attachment the increase of nucleus size at the very early stage of the deposition is limited by the adspecies/clusters attachment on the surface. This is the slow step of the process and the amount of energy that is transferred from the plasma to the surface will be critical for the microcrystalline silicon formation as it can reduce the clustering energy barrier.

A study of the growth and nucleation of a film deposited at 5 Å/s in the center and on the edge of a 30 × 30 cm² substrate shows that the formation of stable nuclei in the center is faster due to the higher frequencies for clustering either by gas phase species or surface species. In addition, the material crystallization starts faster and ends up at higher values in the center of the substrate. Finally, the film morphology in the center and on the edge of the substrate is different and the material on the edge grows rougher mainly due to the smaller average angle of incidence (<90°) of species in this area.

References

- [1] N. Wyrch, et al., Proceedings 2nd World Conference on Photovoltaic Energy Conversion, Vienna, Vol. 1, 1998, p. 467.
- [2] A. Matsuda, *J. Non-Cryst. Solids* 59&60 (1983) 767.
- [3] Y. Yang, M. Katiyar, G.F. Feng, N. Maley, J.R. Abelson, *Appl. Phys. Lett.* 65 (1994) 1769.
- [4] S. Sriraman, S. Agarwal, E.S. Aydil, D. Maroudas, *Nature* 418 (2002) 62.
- [5] I. Solomon, B. Drevillon, E.S. Aydil, *J. Non-Cryst. Solids* 164–166 (1993) 989.
- [6] A. Matsuda, *Thin Solid Films* 337 (1999) 1.
- [7] B. Lyka, E. Amanatides, D. Mataras, *Jap. J. Appl. Phys.* 45 (2006) 8172.
- [8] E. Amanatides, S. Stamou, D. Mataras, *J. Appl. Phys.* 90 (2001) 5786.
- [9] M. Kushner, *J. Appl. Phys.* 63 (1988) 2532.
- [10] J. Perrin, O. Leroy, M.C. Bordage, *Contrib. Plasma Phys.* 36 (1996) 3.
- [11] A. Gross, *Theoretical Surface Science*, Springer-Verlag Berlin Heidelberg, 2009.
- [12] M. Ohring, *Materials Science of thin films*, Elsevier Inc., 2002
- [13] M.M. Visser, J.A. Plaza, D.T. Wang, A.B. Hanneborg, *J. Micromech. Microeng.* 11 (2001) N1.
- [14] M. Pelliccione, T.-M. Lu, *Evolution in Thin Film Morphology*, Springer Berlin Heidelberg, New York, 2008.
- [15] E. Amanatides, D. Mataras, 24th European Photovoltaic Solar Energy Conference, 21–25 September 2009, Hamburg, Germany, 2009, p. 2842.
- [16] M.N. van den Donker, B. Rech, F. Finger, L. Houben, W.M.M. Kessels, M.C.M. van den Sanden, *Prog. Photovolt: Res* 15 (2007) 291.
- [17] M.N. van den Donker, B. Rech, F. Finger, *Appl. Phys. Lett.* 87 (2005) 263503.
- [18] B. Lyka, E. Amanatides, D. Mataras, *J. Non-Cryst. Solids* 352 (2006) 1049.